Published in final edited form as:
Biochemistry. 2011 March 22; 50(11): 1771–1777. doi:10.1021/bi101912q.

Coodination Features and Affinity of the Cu^{2+} Site in the α-Synuclein Protein of Parkinson's Disease

Christopher G. Dudzik[1], **Eric D. Walter**[2], and **Glenn L. Millhauser**[1,*]

[1]Department of Chemistry and Biochemistry, University of California, Santa Cruz, CA 95064

[2]Pacific Northwest Laboratory, P.O. Box 999, K8-98, Richland, WA 99352

Abstract

Parkinson's disease (PD) is the second most prevalent age-related, neurodegenerative disorder, affecting >1% of the population over the age of 60. PD pathology is marked by intracellular inclusions composed primarily of the protein α-synuclein (α-syn). These inclusions also contain copper and the interaction of Cu^{2+} with α-syn may play an important role in PD fibrillogenesis. Here we report the stoichiometry, affinity and coordination structure of the Cu^{2+}-α-syn complex. Electron Paramagnetic Resonance (EPR) titrations show that monomeric α-syn binds 1.0 equivalent of Cu^{2+} at the protein N-terminus. Next, an EPR competition technique demonstrates that α-syn binds Cu^{2+} with a $K_d \approx 0.10$ nM. Finally, EPR and Electron Spin Echo Modulation (ESEEM) applied to a suite of mutant and truncated α-syn constructs reveal a coordination sphere arising from the N-terminal amine, the Asp2 amide backbone and side chain carboxyl group, and the His50 imidazole. The high binding affinity identified here, and in accord with previous measurements, suggests that copper uptake and sequestration may be a part of α-syn's natural function, perhaps modulating copper's redox properties. The findings further suggest that the long-range interaction between the N-terminus and His50 may have a weakening effect on α-syn interaction with lipid membranes thereby mobilizing monomeric α-syn and hastening fibrillogenesis.

Parkinson's disease (PD) is the second most prevalent neurological disorder after Alzheimer's disease, affecting >1% of the US population over the age of 60 (1). PD, an idiopathic neuropathy, is chronic, progressive, and often fatal. Clinical symptoms of PD include diminished motor function, tremors, and speech disorders, attributed to the progressive loss of dopaminergic neurons of the *substantia nigra* (2). A hallmark of affected dopaminergic neurons are Lewy Bodies, cytosolic filamentous inclusions composed primarily of the protein α-synuclein (α-syn). The correlation between α-syn and PD has been clearly demonstrated in animal models where α-syn over expression leads to PD-like motor deficits and intracellular deposits reminiscent of Lewy Bodies (reviewed in (3)). Furthermore, hereditary early onset PD in humans is linked to genetic mutations in α-syn or copy number variation (4,5).

α-Synuclein is a 140 residue, intrinsically disordered protein that is localized primarily to the presynaptic terminals of dopaminergic neurons (Figure 1) (6). The segment referred to as the Non Abeta Component (NAC), residues 61–95, is dominated by hydrophobic residues and tends to form aggregates leading to the parallel beta-sheet rich fibril structures present in Lewy Bodies (7,8). Aggregates from the NAC also contribute approximately 10% of the protein in the senile plaques in Alzheimer's disease patients (9). The N-terminal region of α-

*Address Correspondence to: G. L. Millhauser, voice: (831) 459-2176; fax: (831) 459-2935; glennm@ucsc.edu.

syn, encompassing the NAC (residues 9 – 97), possesses a series of 11-residue imperfect repeats that form an amphipathic alpha-helix when associated with lipid vesicles, a structure similar to exchangeable apolipoproteins (10,11). The C-terminal tail is highly acidic and devoid of secondary structure. However, truncation of this segment produces shortened lag time in fibril kinetics studies, suggesting a possible auto-inhibitory role against α-syn polymerization (12).

While the primary cause of α-syn aggregation in PD is unknown, there is a growing body of evidence implicating environmental factors such as long-term exposure to heavy metals (13–16). The *substantia nigra* region of PD affected brains has been demonstrated to have a significant increase in iron content (17) and Cu^{2+} levels are significantly increased in the Cerebrospinal Fluid (CSF) of PD patients (18). It is well-documented that α-syn interacts with Cu^{2+}, a prevalent species of the CSF, leading to enhanced aggregation and *in vitro* polymerization (19–22).

The interaction between α-syn and Cu^{2+} may also play a role in the protein's normal physiological function. Other neurodegenerative proteins, such as Abeta in Alzheimer's disease and PrP in the prion diseases take up copper (23–25). Unambiguous functions have not yet been identified in these cases, but the regulation of copper homeostasis and redox activity are common themes. Most α-syn is intracellular, where copper is found predominantly in the Cu^{+} state, but a fraction is secreted to the oxidizing extracellular space that favors Cu^{2+} (26). Synaptic Cu^{2+} concentrations range from 2 – 200 μM (27), well in excess of the α-syn-Cu^{2+} affinities measured by most laboratories. Moreover, the *substantia nigra* is part of the *basal ganglia*, which possesses among the highest copper concentrations of the CNS (21,28). Perhaps α-syn is another player in the line of defense against uncomplexed copper, with action localized to the membrane surface. Moreover, Cu^{2+} facilitates oxidation of the N-terminal methionine in α-syn, which hinders in vitro fibril formation (29).

Despite the need to clearly characterize the interaction between α-syn and Cu^{2+}, there is still uncertainty regarding the α-syn-Cu^{2+} binding stoichiometry, affinity and coordination structure (reviewed in (30)). Potentiometric studies performed on α-syn derived N-terminal peptides suggest that Cu^{2+} is coordinated by nitrogens from the N-terminal amine, the Met1 backbone amide, and the His50 imidazole, and an oxygen from the Asp2 carboxylic acid (31,32). These findings are consistent with Trp fluorescence quenching experiments, which also show a preference for copper binding to the N-terminal region (33). Electron paramagnetic resonance (EPR) on full length (140 residue) α-syn suggests a coexistence of structures involving the N-terminus and His50, and that His50 participation may be facile (34). NMR line intensity measurements contrast this and suggest instead that there are no long range coordination structures, but rather a series of local Cu^{2+} sites distributed about the N-terminus, His50, and several areas of negatively charged residues in the C-terminal tail (35).

Reported affinity measurements also yield variation. Circular dichroism titrations identify two Cu^{2+} sites with dissociation constants of 0.7 μM and 60μM (36). Fluorescence quenching probed by a Trp at position four identifies tighter interaction, with a dissociation constant of 100 nM (37). Finally, isothermal titration calorimetry (ITC) of exchange with a soluble copper-glycine complex finds a single Cu^{2+} site in wild type α-syn, with a dissociation constant of approximately 0.2 nM (38).

While most of the studies above point to the involvement of the α-syn N-terminal domain in Cu^{2+} uptake, the role of other protein segments, most notably His50, remain unclear. And as noted above, reported affinity measurements vary by approximately three orders of

magnitude. Here we apply continuous wave (cw) and pulsed EPR to wild type and a panel of mutant α-syn species, at varying stoichiometric ratios. There are three elements to this study. First, through titration studies, we examine the number of Cu^{2+} binding sites, and more generally, how the protein responds to increasing levels of the metal ion. Next, using mutagenesis, we identify the residues responsible for the primary binding sites. Finally, competition studies are applied to evaluate affinity. While our studies support the involvement of the α-syn N-terminal domain, we find strong evidence for participation of His50, especially at 1:1 copper:protein. Moreover, we find that the affinity at this ratio is very high, with a K_d value consistent with the lowest reported value in the current literature, thus pointing to a physiological role for the α-syn-Cu^{2+} interaction.

Materials and Methods

Proteins and Reagents

The human wild type α-syn gene cloned into *pRK172/α-synuclein* plasmid vector was a generous gift from the Fink lab at UCSC. The primers for the mutations H50A and Q98Stop were obtained from Invitrogen. Mutations were performed using the Gene Tailor™ Site Directed Mutagenesis System (Invitrogen Cat. Nos. 12397-014 and 12397-022). α-syn, α-syn(1–97), and α-syn(H50A) were recombinantly expressed in *Escherichia coli* BL21(DE3) competent cells (Invitrogen, Carlsbad, CA) using an auto-induction procedure of Kim et al. described previously (39). Cells were harvested by centrifugation followed by sonication in lysis buffer (50mM NaCl, 20mM Tris, 0.2mM PMSF(phenylmethylsulfonylfluoride), 10%v/v Triton-X100 (Sigma, Switzerland) pH=7.4). Purification was performed using two rounds of ammonium sulfate precipitation (first round 0.164 g/mL; second round 0.117 g/mL) followed by centrifugation, resuspension in 6M guanidine HCl and reverse-phase HPLC (C4 column on a Thermo Scientific instrument). All peptides were synthesized using fluorenylmethoxycarbonyl (Fmoc) methods as described previously (40).

Electron Paramagnetic Resonance

Samples were prepared in degassed buffer containing 25mM MOPS buffer and 25%v/v glycerol, where the glycerol served as a cryoprotectant. All continuous wave X-band spectra (ν = 9.44GHz, microwave power in the range of 0.6–5.0 mW, modulation amplitude of 5.0 G, and sweep width 1200G) were collected at approximately 125K, using a Bruker EleXsys spectrometer and an SHQ (Bruker) cavity equipped with a variable temperature controller. Competition assays were performed as described in text and resultant composite spectra were analyzed using non-negative least-squares (NNLS) in the Matlab program suite. Three-pulse ESEEM measurements were obtained at 20K on a Bruker E580 X-band spectrometer using a dielectric resonator and an Oxford CF 935 cryostat. A π/2-τ-π-*T*-π/2-τ-echo sequence with pulse lengths of 12, 24, and 12 was used. Initial value of τ = 136ns and T was lengthened in 799 steps of 12ns each with 100 samples per step.

Dynamic Light Scattering

Hydrodynamic dimensions were estimated using Dynamic light scattering on a DynaPro Molecular Sizing Instrument (Protein Solutions, Lakewood, NJ) using a1.5-mm path length 12μl quartz cuvette. All experiments were carried out at 35uM protein in 75mM MOPS/NEM buffer at pH=7.4 after 20min centrifugation at 13000rpm.

Results

Stoichiometry

Copper to α-syn binding stoichiometry was determined by EPR titration at pH 7.4 and referenced against a calibrated copper-EDTA standard. Specifically, Cu^{2+} (delivered as

copper acetate) was titrated to a fixed concentration of protein. The integrated cw EPR spectrum (double integral of the 1st derivative EPR signal) is directly proportional to the amount of bound Cu^{2+}. Normalized copper spectra at one, two and four equivalents (Figure 2) are characteristic of a type 2 (oxygen and nitrogen) coordination environment, with well-resolved splittings between the parallel hyperfine lines. At one equivalent of Cu^{2+}, the EPR spectrum gives a single set of hyperfine lines, whereas at two or more equivalents, there is a shift towards lower field, along with the emergence of an additional overlapping spectrum. The implications of these spectra are discussed further below. Spectral integration vs added Cu^{2+}, shown in the inset, demonstrates that copper uptake reaches a maximum at two added equivalents. Consistent with saturation of α-syn at two copper equivalents, we observe no change in spectral details between two and four equivalents.

Although α-syn saturates at 2:1 copper:protein, the integrated spectra reveal only 1.3 bound equivalents (vertical axis of inset in Figure 2). This is in contrast to our previous work with the octarepeat domain of the prion protein, for example, where each added equivalent is directly reflected in the integrated EPR signal. We considered several possible mechanisms that would lead to a lower than expected signal integral. First, with two bound Cu^{2+} ions, there could be diamagnetic coupling between the sites, giving rise to a singlet ground state. This is observed in multinuclear copper complexes and in proteins that have bridging imidazoles between Cu^{2+} centers. The coexistence of singlet and triplet states gives rise to a strong non-Curie temperature dependence. We examined the integral of α-syn with two added equivalents of copper from 20K to 120K (data not shown) and found typical 1/T dependence, which likely rules out coupled copper centers.

Next, we considered whether α-syn, in the presence of copper, formed dimers or well defined oligomers. For example, an α-syn dimer that saturates at three equivalents of copper would give a maximum copper to protein ratio of 1.5, approximately what is observed in the titration of Figure 2. We used Dynamic Light Scattering (DLS) to assess the protein hydrodynamic radius (R_H) and thus whether α-syn remains monomeric in the presence of copper. Experiments were performed with α-syn in buffer, and with one or two equivalents of Cu^{2+} (data not shown). In all cases, a single peak corresponding to a hydrodynamic radius of 3.3 ± 0.2nm dominated, with no evidence of dimers, trimers or other well defined oligomers. Moreover, the measured hydrodynamic radius is consistent with the expected value for a 140 amino acid random coil polypeptide (41).

Finally, we considered whether the second added equivalent is weakly bound and in equilibrium with aquo copper (as EPR silent $Cu(OH)_2$ complexes). To address this possibility, we used the prion-derived peptide HGGGW as a competitor. This well characterized species binds Cu^{2+} with a dissociation constant of 7.0 μM. Addition of 1.0 eq. of HGGGW to a 1.5:1 mixture of Cu^{2+}:α-syn completely eliminated the α-syn EPR spectrum associated with the second Cu^{2+} equivalent. In its place we observed the characteristic spectrum of the Cu^{2+}-HGGGW complex and, to within experimental error, spectral integration accounted for 1.5 eq. of Cu^{2+}. Consequently, the peptide HGGGW efficiently competes away the second Cu^{2+} eq. from α-syn demonstrating a low affinity interaction characterized by a $K_d \gg 7$ μM. We conclude from these experiments that while α-syn takes up two eq. of Cu^{2+}, the second eq. binds with low affinity and is not physiologically important. These results are in good agreement with recent findings by Hong and Simon who used isothermal titration calorimetry to identify a single high affinity copper site in α-syn (38).

Identification of the Cu^{2+} Coordination Features

To determine the smallest segment of wt α-syn that possesses all the functional groups that directly coordinate Cu^{2+}, we developed a panel of truncated and chemically modified α-syn

variants. These include α-syn(1–10), α-syn(1–56), α-syn(1–97), and several N-terminal acetylated species. At a single equivalent of Cu^{2+}, α-syn(1–56) and α-syn(1–97) give spectra that nearly overlap with wild type (Figure 3). However, upon addition of a second Cu^{2+} equivalent, only α-syn(1–97) shows a shift in the parallel region similar to that observed in full-length α-syn. In contrast, while α-syn(1–10) takes up a single equivlent of Cu^{2+}, the bound species gives an EPR spectrum that does not overlap with 1:1 Cu^{2+}: α-syn(1–97) or 1:1 with full-length. Acetylation of any of the α-syn variants completely abrogates copper uptake (data not shown). Together, these data demonstrate that the α-syn N-terminus participates in Cu^{2+} coordination, (42) but residues beyond the first ten are required to recapitulate the coordination environment of wild type α-syn.

To identify the specific residues required for copper coordination, point mutations were introduced into both synthetically produced peptides and recombinantly expressed α-syn protein. $A_{\|}$ and $g_{\|}$ values derived from the EPR spectra (shown in Table 1), are consistent with a 3N1O coordination environment, as determined from Peisach-Blumberg correlations. In addition, previous potentiometric studies suggest that Asp2 is involved in Cu(II) binding (31,32). Indeed, peptide coordination of metal centers with the 2nd aspartate residue following a free peptide N-terminus give very stable Cu^{2+} complexes (43). To directly test for this, we prepared α-syn(1–56) with a D2A point mutation. EPR spectra 1:1 Cu^{2+} complexes with α-syn(1–56) and α-syn(1–56, D2A) reveal differences in the intense perpendicular features at approximately 3300 G and in the parallel hyperfine splittings, in turn suggesting a direct interaction with the aspartate side chain.

Next we considered His50. Although distal from the α-syn N-terminus, imidazole is an avid copper binding group and experiments above suggest participation from residues beyond the first ten. EPR spectra from wild type α-syn and α-syn(H50A), each with a single eq. of Cu^{2+}, were compared as shown in Fig. 3. The parallel region for the mutant species exhibits great splitting (larger $A_{\|}$) consistent with replacement of an equatorial nitrogen with an oxygen. Moreover, this spectrum does not overlap with that of wild type with either 1.0 or 2.0 eq. Cu^{2+}.

To further assess the involvement of H50 in Cu^{2+} coordination, we used Electron Spin-Echo Envelope Modulation (ESEEM). ESEEM is a pulsed EPR technique with sensitivity to spin-active nuclei approximately 10 Å of the paramagnetic copper center (44). At X-band frequencies, the distal ^{14}N (I = 1) of a coordinated imidazole ring gives characteristic quadrupolar transitions and is diagnostic for interacting His side chains (45). The FT ESEEM of α-syn with 1.0 eq. Cu^{2+} shown in figure 4 is typical for imidazole, with three low frequency peaks that correspond to transitions among ^{14}N quadropolar levels in exact cancellation, as well as the ≈ 4 MHz peak from the non-canceled electron spin manifold. We also find that the α-syn(H50A) fails to give an ESEEM spectrum with 1.0 eq. Cu^{2+}. Together, these findings demonstrate unequivocally the equatorial coordination by the H50 imidazole (40). The spectra in figure 4 further show that the H50 coordinates Cu^{2+} in wild type α-syn and in truncated α-syn(1–97) even in the presence of excess metal ion. Addition of 2.0 Cu^{2+} eq., however, brings out additional low intensity peaks at approximately 2 and 2.8 MHz. Past work from our lab on the octarepeat domain of the prion protein demonstrated that these lines can arise from the ^{14}N of an amide group coordinated through the carboxyl oxygen, as shown in the spectrum for Cu^{2+}-HGGGW (40). The appearance of these transitions in α-syn suggests that the weakly bound second Cu^{2+} eq. coordinates in a similar fashion.

Additional tests were performed to evaluate whether the H50 segment alone of α-syn alone is capable of taking up Cu^{2+} with high affinity. We prepared an acetylated 21 residue peptide corresponding to a segment of α-syn with H50 in the center (α-syn(39–60)).

Titration up to 1.0 eq. Cu^{2+} gave a very weak EPR spectrum (reflecting < 10% of added copper) inconsistent with a bound species.

Binding Affinity

To evaluate the dissociation constant, K_d, of the Cu^{2+}-α-syn complex, we used an EPR competition technique previously developed in our lab (46). High affinity competitors that take up Cu^{2+} with a 1:1 stoichiometry are added to a Cu^{2+}/α-syn solution. Both oxidized glutathione and pentaglycine peptides are well characterized chelators and give Cu^{2+} EPR spectra that are distinct from that of the Cu^{2+}-α-syn complex. Spectral decomposition gives the ratio of copper bound to α-syn and specific competitor. Analysis using the known K_d of the competitor determines the α-syn dissociation constant. With this approach, the amount of competitor may be varied to insure that both bound species give resolvable EPR spectra of similar signal strengths. Table 2 shows that wt α-syn binds one equivalent of Cu^{2+} with a K_d of either 0.11 nM or 0.15 nM, as determined from independent experiments with pentaglycine or oxidized glutathione, respectively. These values are approximately five orders of magnitude lower than the > 7 uM K_d found for the second equivalent, as described above. Consequently, these data further support the finding that α-syn takes up only a single eq. of Cu^{2+} with high affinity. To test for H50 coordination, we also performed competition experiments on the α-syn H50A mutant. As determined from both competitors, this species exhibits an approximately four-fold lower affinity than wild type.

Discussion

Our EPR experiments demonstrate that the Cu^{2+} coordination environment in α-syn involves the N-terminal amine and the carboxylate side chain of Asp2. In addition, ESEEM reveals participation by the H50 imidazole. To account for 3N1O coordination, suggested by evaluation of the magnetic tensor values, we propose involvement of the Asp2 backbone amide nitrogen. In further supporting this assignment, the lack of amide ^{14}N couplings in the ESEEM spectra rule against Met1 backbone carbonyl coordination (40). Our findings at pH 7.4, suggest a well-defined coordination environment without evidence of structural heterogeneity. The coordination features are shown in Figure 5. Involvement of the N-terminal residues is consistent with studies from peptide based Cu^{2+} coordination complexes with an Asp as the second amino acid (43). And while α-syn may take up a second Cu^{2+} equivalent, the interaction is low affinity and likely unimportant to physiological function. In addition, we find that the dissociation constant for the first equivalent is approximately 0.10 nM.

Certain aspects of our findings support previously published work. For example, potentiometric measurements performed on α-syn segments suggest a similar coordination environment, marked by a pH sensitivity expected for N-terminal and backbone nitrogens, and a carboxylate group (31,32). Site specific tryptophan fluorescence studies identify a 1:1 α-syn:Cu^{2+} complex with the N-terminal segment as the primary anchor point (33). Electrospray mass spectrometry also finds a single N-terminal site (47), wheras MALDI finds evidence of two Cu^{2+} binding sites with significantly different affinities, the tighter of which (sub micromolar) located to the N-terminus (36). Previous EPR experiments at pH 5.0 and 7.4 were interpreted to suggest a coexistence of two coordination spheres at the higher pH, distinguished by involvement of His50 (34). While our findings certainly agree with the His-bound species, we do not find evidence for a second pH 7.4 coordination mode. The four-fold enhanced affinity we find for wild type α-syn vs the α-syn(H50A) mutant further supports imidazole coordination, and we do not find features of the α-syn(1–10) or α-syn(H50A) EPR spectra superimposed on wildtype.

Despite emerging consensus on the molecular details of the Cu^{2+} coordination sphere, there remains wide disagreement with regard to affinity. As noted in the Introduction, published values for the dissociation constant range from micromolar to nanomolar. Recently, Hong and Simon used a refined ITC approach whereby Cu^{2+} is added as a glycine complex (38). With appropriate treatment of the complex equilibria, they determine an association constant based on heat release through a copper titration. Wild type α-syn at pH 7.4 gives an association constant of $4.7 \times 10^9\ M^{-1}$, corresponding to a K_d of 0.21 nM. Moreover, they find no evidence of a second Cu^{2+} coordination site. These results are in remarkable agreement with ours described here and support a very high affinity, mononuclear site with principal anchor points at the protein N-terminus.

The emerging biophysical evidence strongly suggests that α-syn interacts with Cu^{2+} *in vivo*. The residues involved in copper chelation are highly conserved, and the protein is abundant within the cell and localized to membrane surfaces at the synaptic cleft where CSF Cu^{2+} levels exceed micromolar concentrations (26,48,49). The sub-nanomolar α-syn-Cu^{2+} K_d, along with the abundance of synaptic α-syn, suggests that any Cu^{2+} localized to the extracellular membrane would be tightly complexed. Recent evidence suggests that copper bound to α-syn within neurons of the *substantia nigra* is stabilized in the +2 oxidation state (50). An intriguing possibility then is that perhaps α-syn sequesters Cu^{2+} at the membrane and modulates copper's inherent redox activity. Electrochemical experiments demonstrate that the Cu^{2+}-α-syn undergoes redox cycling, but favors the production of hydrogen peroxide, which is less damaging to cells than radical species often produced by weakly complexed copper (47).

The interaction of α-syn intra-cellular with synaptic vesicles is well documented, and new evidence shows that wt α-syn interacts with SNARE complexes, perhaps as a chaperone, participating in membrane fusion (51–53). Although membrane-associated α-syn is largely helical, an extended α-helix structure is incompatible with the polypeptide wrapping back to coordinate Cu^{2+} with the N-terminus and His50. We propose, therefore, that Cu^{2+} provides a mechanism for α-syn release from the synaptic vesicle membrane, upon exposure to the extracellular environment, switching from the membrane-induced helical structure to the Cu^{2+}-bound structure shown in Figure 5. This same mechanism may also operate in PD. A copper mediated weakening of the interaction between α-syn and cellular membranes could increase the soluble protein fraction thus hastening fibrillogenesis.

In summary, α-syn interacts strongly with Cu^{2+} *in vitro*. Whether this interaction is part of the protein's natural function, a component in the disease process, or both, is the subject for further study. Our results show that monomeric α-syn binds one equivalent of Cu^{2+} with ≈ 0.1 nM affinity. This binding mode creates a protein conformational change bringing the N-terminus and H50 in close proximity. Any additional Cu^{2+} association with the protein is weak, non-specific and not physiologically relevant. Future work will focus on determining the role of this interaction on α-syn cycling at the cell surface, and the consequences in PD pathogenesis.

Acknowledgments

The authors are very grateful to Drs. Stefen Stoll and David Britt, UC Davis, for their valuable consultation on the collection and processing of the ESEEM spectra.

This work was supported by NIH grant GM065790.

Abbreviations

α-syn	human α-synuclein
CNS	Central Nervous System
CSF	Cerebral Spinal Fluid
DLS	Dynamic Light Scattering
EPR	Electron Paramagnetic Resonance
ESEEM	Electron Spin Echo Envelope Modulation
K_d	Dissociation Constant
LB	Lewy Bodies
NAC	Non-Abeta Component
PD	Parkinson's Disease

Literature Cited

1. Lees AJ, Hardy J, Revesz T. Parkinson's disease. Lancet. 2009; 373:2055–2066. [PubMed: 19524782]
2. Jankovic J. Parkinson's disease: clinical features and diagnosis. J Neurol Neurosurg Psychiatry. 2008; 79:368–376. [PubMed: 18344392]
3. Dawson TM, Ko HS, Dawson VL. Genetic animal models of Parkinson's disease. Neuron. 66:646–661. [PubMed: 20547124]
4. Chartier-Harlin MC, Kachergus J, Roumier C, Mouroux V, Douay X, Lincoln S, Levecque C, Larvor L, Andrieux J, Hulihan M, Waucquier N, Defebvre L, Amouyel P, Farrer M, Destee A. Alpha-synuclein locus duplication as a cause of familial Parkinson's disease. Lancet. 2004; 364:1167–1169. [PubMed: 15451224]
5. Vila M, Przedborski S. Genetic clues to the pathogenesis of Parkinson's disease. Nat Med. 2004; 10 Suppl:S58–S62. [PubMed: 15272270]
6. Yang ML, Hasadsri L, Woods WS, George JM. Dynamic transport and localization of alpha-synuclein in primary hippocampal neurons. Mol Neurodegener. 2010; 5:9. [PubMed: 20181133]
7. Chen M, Margittai M, Chen J, Langen R. Investigation of alpha-synuclein fibril structure by site-directed spin labeling. J Biol Chem. 2007; 282:24970–24979. [PubMed: 17573347]
8. Wirths O, Bayer TA. Alpha-synuclein, Abeta and Alzheimer's disease. Prog Neuropsychopharmacol Biol Psychiatry. 2003; 27:103–108. [PubMed: 12551731]
9. Lucking CB, Brice A. Alpha-synuclein and Parkinson's disease. Cell Mol Life Sci. 2000; 57:1894–1908. [PubMed: 11215516]
10. Jao C, Hegde B, Chen J, Haworth I, Langen R. Structure of membrane-bound α-synuclein from site-directed spin labeling and computational refinement. Proceedings of the National Academy of Sciences. 2008; 105:19666.
11. Davidson WS, Jonas A, Clayton DF, George JM. Stabilization of alpha-synuclein secondary structure upon binding to synthetic membranes. J Biol Chem. 1998; 273:9443–9449. [PubMed: 9545270]
12. Zhou W, Long C, Reaney SH, Di Monte DA, Fink AL, Uversky VN. Methionine oxidation stabilizes non-toxic oligomers of alpha-synuclein through strengthening the auto-inhibitory intra-molecular long-range interactions. Biochim Biophys Acta. 1802:322–330. [PubMed: 20026206]
13. Rybicki BA, Johnson CC, Uman J, Gorell JM. Parkinson's disease mortality and the industrial use of heavy metals in Michigan. Mov Disord. 1993; 8:87–92. [PubMed: 8419812]
14. Singh C, Ahmad I, Kumar A. Pesticides and metals induced Parkinson's disease: involvement of free radicals and oxidative stress. Cell Mol Biol (Noisy-le-grand). 2007; 53:19–28. [PubMed: 17543230]

15. Barnham KJ, Bush AI. Metals in Alzheimer's and Parkinson's diseases. Curr Opin Chem Biol. 2008; 12:222–228. [PubMed: 18342639]
16. Bisaglia M, Tessari I, Mammi S, Bubacco L. Interaction Between α-Synuclein and Metal Ions, Still Looking for a Role in the Pathogenesis of Parkinson's Disease. Neuromol Med. 2009; 11:239–251.
17. Dexter DT, Carayon A, Javoy-Agid F, Agid Y, Wells FR, Daniel SE, Lees AJ, Jenner P, Marsden CD. Alterations in the levels of iron, ferritin and other trace metals in Parkinson's disease and other neurodegenerative diseases affecting the basal ganglia. Brain. 1991; 114(Pt 4):1953–1975. [PubMed: 1832073]
18. Pall H, Blake D, Gutteridge J, Williams A, Lunec J, Hall M, Taylor A. Raised cerebrospinal-fluid copper concentration in Parkinson's disease. The Lancet. 1987; 330:238–241.
19. Bush AI. Metals and neuroscience. Curr Opin Chem Biol. 2000; 4:184–191. [PubMed: 10742195]
20. Alimonti A, Bocca B, Pino A, Ruggieri F, Forte G, Sancesario G. Elemental profile of cerebrospinal fluid in patients with Parkinson's disease. J Trace Elem Med Biol. 2007; 21:234–241. [PubMed: 17980814]
21. Desai V, Kaler SG. Role of copper in human neurological disorders. Am J Clin Nutr. 2008; 88 855S–858S.
22. Uversky VN, Li J, Fink AL. Metal-triggered structural transformations, aggregation, and fibrillation of human alpha-synuclein. A possible molecular NK between Parkinson's disease and heavy metal exposure. J Biol Chem. 2001; 276:44284–44296. [PubMed: 11553618]
23. Millhauser GL. Copper and the prion protein: methods, structures, function, and disease. Annu Rev Phys Chem. 2007; 58:299–320. [PubMed: 17076634]
24. Sarell CJ, Syme CD, Rigby SE, Viles JH. Copper(II) binding to amyloid-beta fibrils of Alzheimer's disease reveals a picomolar affinity: stoichiometry and coordination geometry are independent of Abeta oligomeric form. Biochemistry. 2009; 48:4388–4402. [PubMed: 19338344]
25. Millhauser GL. Copper Binding in the Prion Protein. Acc. Chem. Res. 2004; 37:79–85. [PubMed: 14967054]
26. Que EL, Domaille DW, Chang CJ. Metals in neurobiology: probing their chemistry and biology with molecular imaging. Chemical Reviews. 2008; 108:1517–1549. [PubMed: 18426241]
27. Chattopadhyay M, Walter ED, Newell DJ, Jackson PJ, Aronoff-Spencer E, Peisach J, Gerfen GJ, Bennett B, Antholine WE, Millhauser GL. The octarepeat domain of the prion protein binds Cu(II) with three distinct coordination modes at pH 7.4. J Am Chem Soc. 2005; 127:12647–12656. [PubMed: 16144413]
28. Madsen E, Gitlin JD. Copper and iron disorders of the brain. Annu Rev Neurosci. 2007; 30:317–337. [PubMed: 17367269]
29. Lucas HR, Debeer S, Hong MS, Lee JC. Evidence for copper-dioxygen reactivity during alpha-synuclein fibril formation. J. Am. Chem. Soc. 132:6636–6637. [PubMed: 20423081]
30. Brown DR. Interactions between metals and alpha-synuclein--function or artefact? FEBS J. 2007; 274:3766–3774. [PubMed: 17617226]
31. Kowalik-Jankowska T, Rajewska A, Jankowska E, Grzonka Z. Copper(II) binding by fragments of alpha-synuclein containing M1-D2- and -H50-residues; a combined potentiometric and spectroscopic study. Dalton Trans. 2006:5068–5076. [PubMed: 17060993]
32. Kowalik-Jankowska T, Rajewska A, Wisniewska K, Grzonka Z, Jezierska J. Coordination abilities of N-terminal fragments of alpha- synuclein towards copper(II) ions: a combined potentiometric and spectroscopic study. J Inorg Biochem. 2005; 99:2282–2291. [PubMed: 16203037]
33. Lee JC, Gray HB, Winkler JR. Copper(II) binding to alpha-synuclein, the Parkinson's protein. J Am Chem Soc. 2008; 130:6898–6899. [PubMed: 18465859]
34. Drew SC, Leong SL, Pham CL, Tew DJ, Masters CL, Miles LA, Cappai R, Barnham KJ. Cu2+ binding modes of recombinant alpha-synuclein--insights from EPR spectroscopy. J Am Chem Soc. 2008; 130:7766–7773. [PubMed: 18494470]
35. Sung YH, Rospigliosi C, Eliezer D. NMR mapping of copper binding sites in alpha-synuclein. Biochim Biophys Acta. 2006; 1764:5–12. [PubMed: 16338184]
36. Binolfi A, Lamberto GR, Duran R, Quintanar L, Bertoncini CW, Souza JM, Cervenansky C, Zweckstetter M, Griesinger C, Fernandez CO. Site-specific interactions of Cu(II) with alpha and

beta-synuclein: bridging the molecular gap between metal binding and aggregation. J Am Chem Soc. 2008; 130:11801–11812. [PubMed: 18693689]

37. Jackson MS, Lee JC. Identification of the minimal copper(II)-binding alpha-synuclein sequence. Inorg Chem. 2009; 48:9303–9307. [PubMed: 19780617]
38. Hong L, Simon JD. Binding of Cu(II) to human alpha-synucleins: comparison of wild type and the point mutations associated with the familial Parkinson's disease. J Phys Chem B. 2009; 113:9551–9561. [PubMed: 19548659]
39. Kim M, Elvin C, Brownlee A, Lyons R. High yield expression of recombinant pro-resilin: lactose-induced fermentation in E. coli and facile purification. Protein Expr Purif. 2007; 52:230–236. [PubMed: 17166741]
40. Burns CS, Aronoff-Spencer E, Dunham CM, Lario P, Avdievich NI, Antholine WE, Olmstead MM, Vrielink A, Gerfen GJ, Peisach J, Scott WG, Millhauser GL. Molecular features of the copper binding sites in the octarepeat domain of the prion protein. Biochemistry. 2002; 41:3991–4001. [PubMed: 11900542]
41. Uversky VN, Li J, Souillac P, Millett IS, Doniach S, Jakes R, Goedert M, Fink AL. Biophysical properties of the synucleins and their propensities to fibrillate: inhibition of alpha-synuclein assembly by beta- and gamma-synucleins. J Biol Chem. 2002; 277:11970–11978. [PubMed: 11812782]
42. Sigel H, Martin BR. Coordinating Properties of the Amide Bond. Stability and Structure of Metal Ion Complexes of Peptides and Related Ligands. Chemical Reviews. 1982; 82:385–426.
43. Kallay C, Varnagy K, Micera G, Sanna D, Sovago I. Copper(II) complexes of oligopeptides containing aspartyl and glutamyl residues. Potentiometric and spectroscopic studies. J Inorg Biochem. 2005; 99:1514–1525. [PubMed: 15927267]
44. Dikanov, SA.; Tsvetkov, YD. Electron spin-echo envelope modulation (ESEEM) spectroscopy. Boca Raton, FL: CRC press; 1992.
45. Mims WB, Peisach J. The nuclear modulation effect in electron spn echoes for complexes of Cu(II) and imidazole with 14N and 15N. J. Chem. Phys. 1978; 69:4921–4930.
46. Walter ED, Chattopadhyay M, Millhauser GL. The affinity of copper binding to the prion protein octarepeat domain: evidence for negative cooperativity. Biochemistry. 2006; 45:13083–13092. [PubMed: 17059225]
47. Wang C, Liu L, Zhang L, Peng Y, Zhou F. Redox reactions of the alpha-synuclein-Cu(2+) complex and their effects on neuronal cell viability. Biochemistry. 2010; 49:8134–8142. [PubMed: 20701279]
48. Kanabrocki EL, Case LF, Miller EB, Kaplan E, Oester YT. A Study of Human Cerebrospinal Fluid: Copper and Manganese. J Nucl Med. 1964; 5:643–648. [PubMed: 14212189]
49. Millhauser GL. Copper and the Prion Protein: Methods, Structures, Function, and Disease. 2010:1–24.
50. Chwiej J, Adamek D, Szczerbowska-Boruchowska M, Krygowska-Wajs A, Bohic S, Lankosz M. Study of Cu chemical state inside single neurons from Parkinson's disease and control substantia nigra using the micro-XANES technique. J Trace Elem Med Biol. 2008; 22:183–188. [PubMed: 18755393]
51. Chandra S, Gallardo G, Fernandez-Chacon R, Schluter OM, Sudhof TC. Alpha-synuclein cooperates with CSPalpha in preventing neurodegeneration. Cell. 2005; 123:383–396. [PubMed: 16269331]
52. Bonini NM, Giasson BI. Snaring the function of alpha-synuclein. Cell. 2005; 123:359–361. [PubMed: 16269324]
53. Burre J, Sharma M, Tsetsenis T, Buchman V, Etherton MR, Sudhof TC. Alpha-synuclein promotes SNARE-complex assembly in vivo and in vitro. Science. 2010; 329:1663–1667. [PubMed: 20798282]

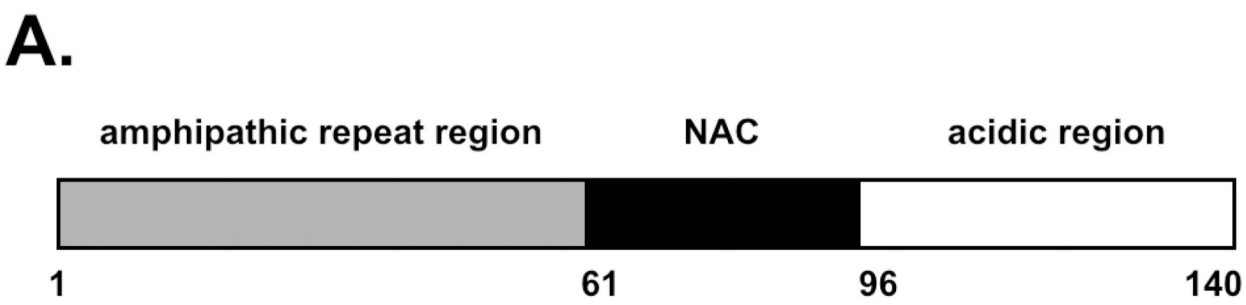

B.

α-syn(1-60) amphipathic repeat region

MDVFMKGLSKAKEGVVAAAEKTKQGVAEAAGKTKEGVLYVGSKTKEGVVHGVATVAEKTK

α-syn(61-95) NAC (non-amyloid component)

EQVTNVGGAVVTGVTAVAQKTVEGAGSIAAATGFV

α-syn(96-140) acidic region

KKDQLGKNEEGAPQEGILEDMPVDPDNEAYEMPSEEGYQDYEPEA

Figure 1.

Features of the α-synuclein primary structure identifying (A) the three consensus segments and (B) the amino acid sequence associated with each segment. Residues 9 – 97, encompassing the amphipathic repeat region and the NAC, forms an extended helix when associated with lipid membranes.

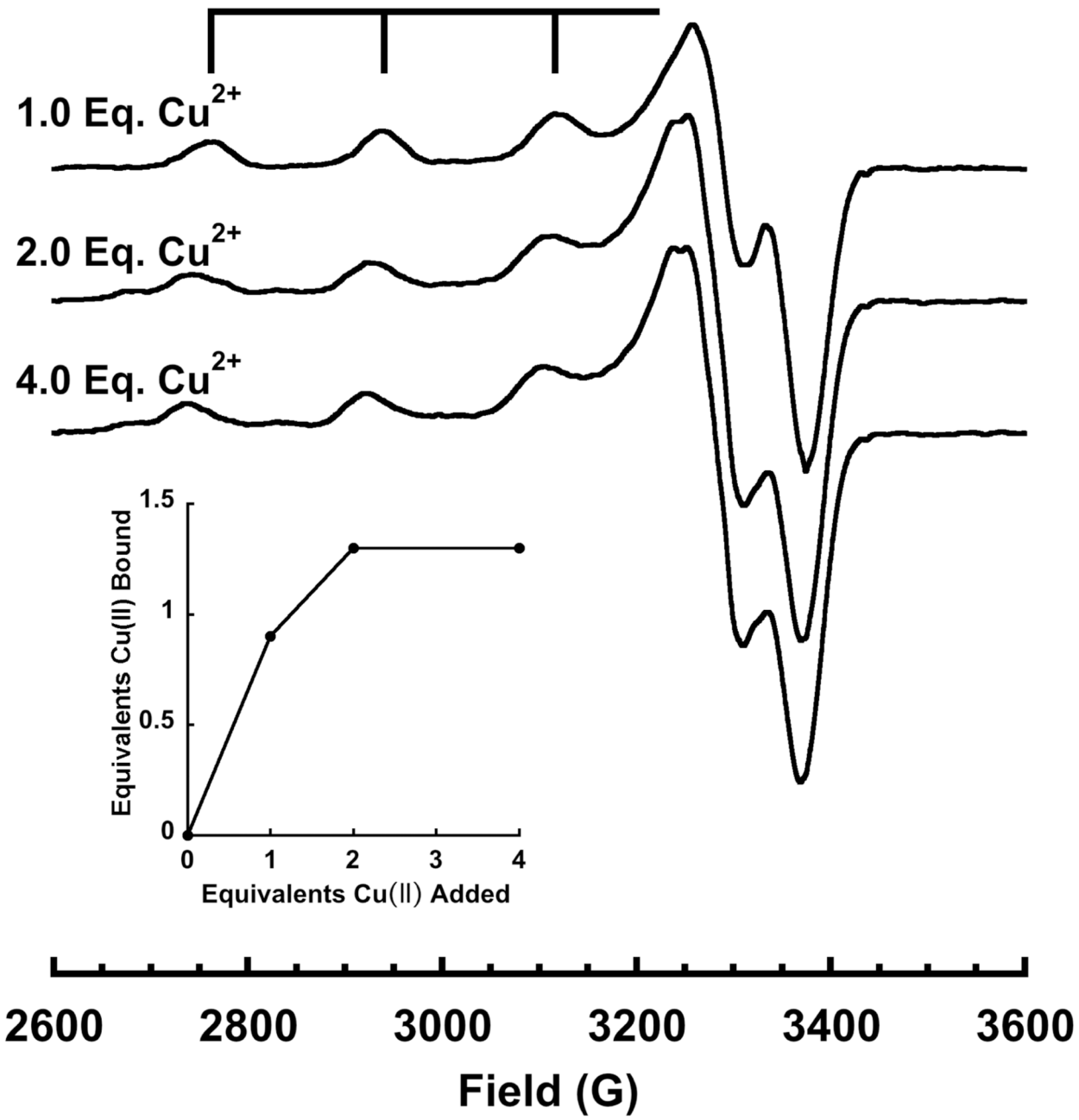

Figure 2.

X-band EPR spectra of α-syn at pH=7.4 with 1, 2, and 4 equivalents of Cu^{2+}. Specra were collected at 111 K, ν = 9.44GHz, with a sweep width of 1200 G. The inset shows EPR detected Cu^{2+} as a function of added Cu^{2+} and demonstrates saturation at approximately 2.0 eq. However, competition studies find that the second equivalent is weakly coordinated.

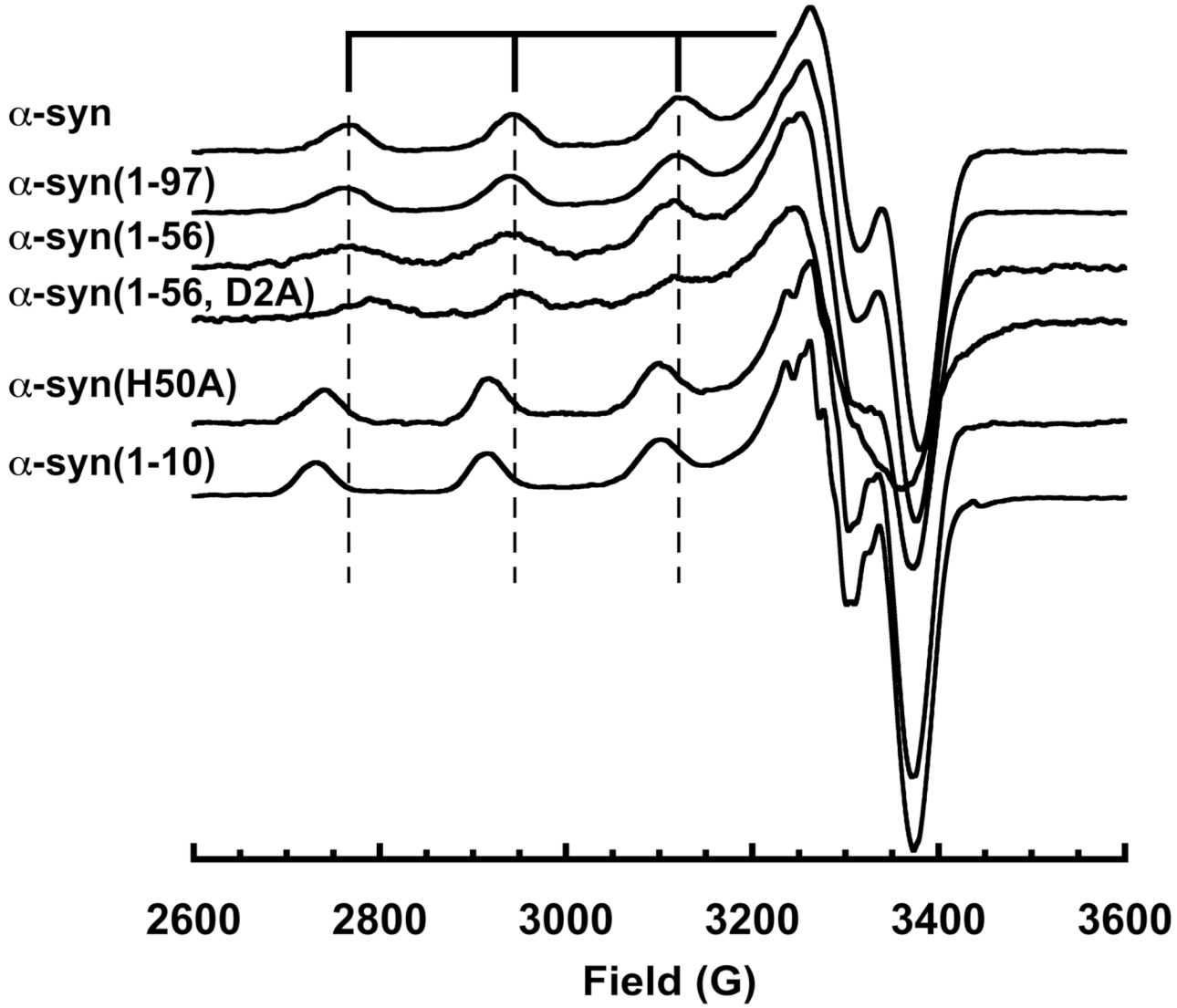

Figure 3.
X-Band EPR spectra of α-syn, mutants and truncated species. Vertical lines correspond to the parallel hyperfine features of wild type α-syn. α-Syn(1–97) gives a spectrum that superimposes on wild type, but all other species show significant variation. α-Syn(1–10) and α-syn(H50A) gives equivalent spectra, but distinct from wild type, demonstrating involvement of His50 in the coordination sphere.

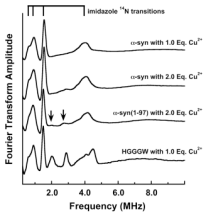

Figure 4.

Three pulse ESEEM spectra of α-syn with 1.0 Eq. Cu^{2+} and 2.0 Eq. Cu^{2+}, α-syn(1–97) with 2.0 Eq. Cu^{2+} and prion protein sequence HGGGW with 1.0 Eq. Cu^{2+}. These spectra reveal the expected quadrupolar transitions associated with an imidazole remote nitrogen and demonstrate coordination by His50. α-syn(H50A) fails to give an ESEEM spectrum. α-Syn(1–97) with 2.0 Eq. Cu^{2+} gives additional weak features at 2.0 and 2.8 MHz (arrows), similar to peaks observed in HGGGW and assigned to an amide nitrogen coordinated through the backbone carbonyl.

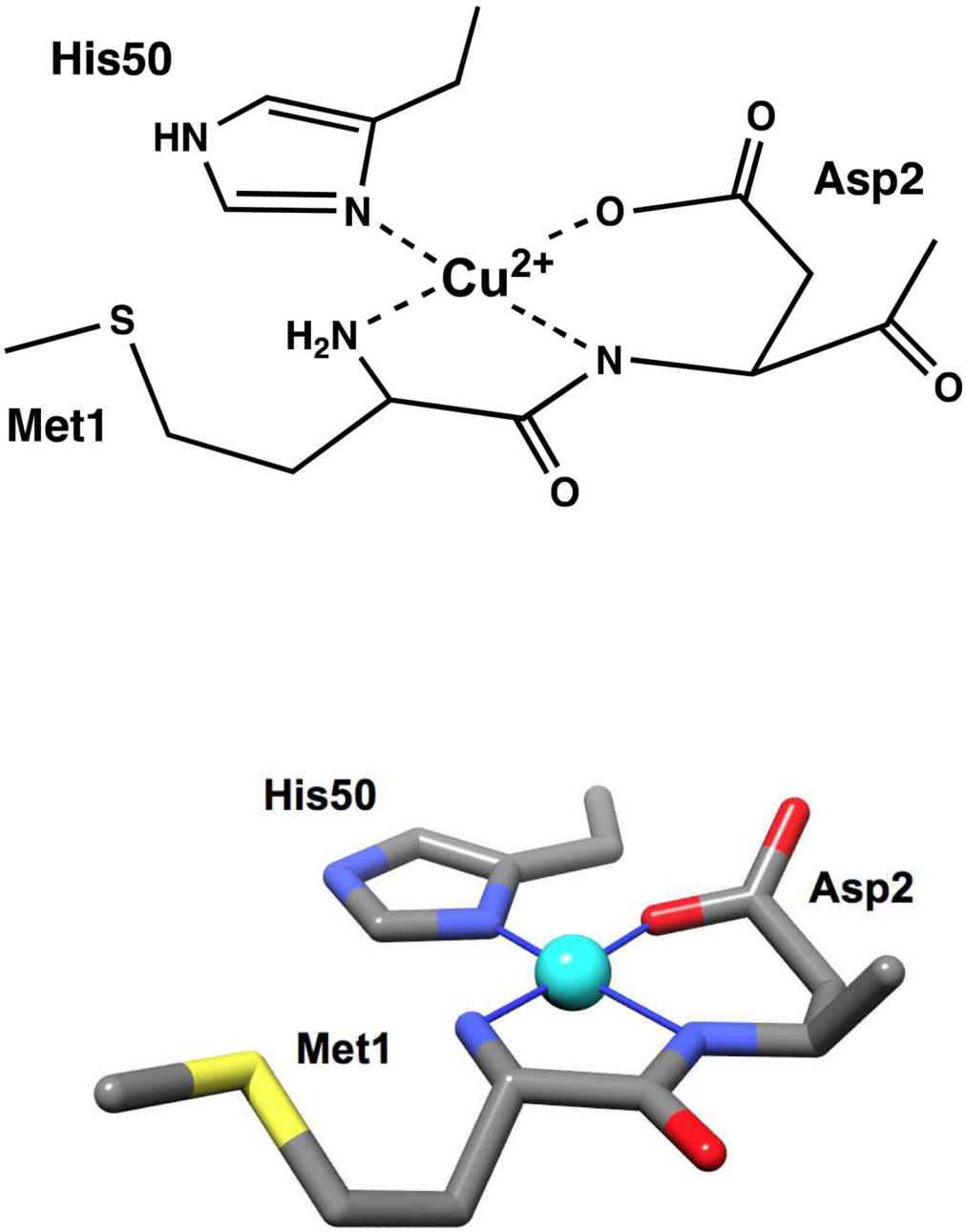

Figure 5.
Coordination features of the primary Cu^{2+} site in α-syn identified here in bond line (top) and stick (bottom) models. Competition studies show that this complex exhibits a dissociation constant of approximately 0.1 nM.

Table 1

EPR Parameters

Protein	g∥	A∥ (G)
α-synuclein	2.226	178.6
α-syn(1–10)	2.245	183.3
α-syn(1–56)	2.229	173.2
α-syn(1–97)	2.226	178.6
α-syn(H50A)	2.242	176.6

Table 2

Dissociation Constants (nM) Determined from Competition Studies

Protein/Competitor	Pentaglycine (K_d = 40 nM)	Oxidized Glutathione[a] (K_d = 0.066 nM)
α-synuclein	0.11 ± 0.03	0.15
α-syn(H50A)	0.40 ± 0.01	0.60

[a] K_d determinations using oxidized glutathione were performed once, and do not have standard errors.